

Uplift of Anatolia

Aral I. OKAY^{1,2,*}, Massimiliano ZATTIN³, Ercan ÖZCAN², Gürsel SUNAL²

¹Eurasia Institute of Earth Sciences, İstanbul Technical University, İstanbul, Turkey

²Department of Geological Engineering, Faculty of Mines, İstanbul Technical University, İstanbul, Turkey

³Department of Geosciences, University of Padua, Padua, Italy

Received: 16.03.2020 • Accepted/Published Online: 29.05.2020 • Final Version: 01.07.2020

Abstract: The Cenozoic history of the Anatolian Plateau is investigated using the distribution of the last Cenozoic marine strata, the ages of Neogene continental sediments and magmatic rocks, and thermochronology. In central and northern Anatolia, the youngest marine sediments are of Middle Eocene age and show that the region has been above the sea level since ca. 41 Ma. The preservation of marine Eocene sequences over large regions and widespread distribution of Neogene continental sediments point to minor erosion or subsidence, except in the Miocene core complexes, and indicate average surface uplift or subsidence rates of less than 0.05 km/Myr since 41 Ma. The Cenozoic mammal ages point to widespread continental deposition on the Anatolian Plateau from Early Miocene (ca. 22 Ma) to the present, and a similar pattern of semicontinuous magmatism has been observed in Anatolia since ca. 23 Ma. New thermochronological data from central Anatolia to west of Ankara have indicate a major exhumation phase during the Paleocene and Early Eocene, followed by minor uplift and/or subsidence. Miocene exhumation is restricted to the core complexes, such as the Kazdağ Massif. The Anatolian Plateau has been a land area since 41 Ma and was characterized by continental sedimentation and volcanism in the last 22 Myr. In this period, subsidence and uplift were balanced so that central Anatolia was maintained above sea level. In contrast, its southern mountainous margin, the Taurides, is free of Neogene magmatism and has undergone a fast uplift above sea level since 8 Ma (ca. 0.3 km/Myr). These differences indicate that the uplift of Anatolia cannot be ascribed to a single mechanism. Flat subduction, followed by mantle upwelling under Anatolia in the post-Middle Eocene period, maintained the region above the sea level, whereas the Late Miocene rupture of the subducting eastern Mediterranean oceanic slab have induced fast uplift of the Taurides.

Key words: Anatolian Plateau, uplift, exhumation, thermochronology, Cenozoic, mammal ages

1. Introduction

Plateaus are major physiographic structures on the Earth that influence tectonics, sedimentation, hydrography, and climate. Their mode of formation and duration are significant geological problems. The Central Anatolian Plateau, with a surface area of 800 km by 400 km, an average height of ~1 km, and low relief (<300 m), is one of the world's major plateaus (Figure 1). In the north and south, it is bounded by the higher elevation Pontide and Tauride mountains, respectively (e.g., Cosentino et al., 2012). It lies between the higher elevation (~2 km) East Anatolian Highlands, which has been undergoing active shortening between the colliding Arabian and Eurasian plates, and the lower elevation extensional Aegean province (e.g., Reilinger et al., 2006). The recent fast uplift of the Taurides is now well constrained, and is linked to delamination and/or slab breakoff during the Late Miocene (e.g., Schildgen et al., 2014). Various post-Late Miocene (<8 Ma) subcrustal processes are invoked for the formation of the Central Anatolia Plateau (e.g., Bartol and Govers, 2014; Göğüş et al., 2017); however,

there are few data on its timing. Here, the formation of the Anatolian Plateau was investigated using four data sets: a) the ages of the last marine strata, b) the ages of the continental Neogene sequences, c) the age of Cenozoic magmatism, and d) thermochronology. New thermochronological data from central Anatolia are also provided.

There have been several recent studies on the Quaternary surface uplift in Anatolia, generally based on surface dating of marine or fluvial terraces (e.g., Yıldırım et al., 2013; Çiner et al., 2015; Berndt et al. 2018). The data from these studies covered the last few hundred thousand years and are local. They are difficult to extrapolate back to several tens of millions of years and to all of Anatolia; therefore, they are not used in this study.

2. Methods

This study involved the compilation and critical evaluation of a large number of published papers, as well as collection of new thermochronological data from central Anatolia.

* Correspondence: okay@itu.edu.tr



Figure 1. Physiography of the Anatolian Plateau and the surrounding region. NAF: North Anatolian fault, EAF: East Anatolian Fault. The base map is from GeoMapApp (<http://www.geomapapp.org/>).

2.1. Data compilation

We compiled the published ages of the last Cenozoic marine deposits in Anatolia (Table S1), of the continental Cenozoic sediments (Tables S2 and S3), and Cenozoic volcanism (Table S4) in Turkey, and thermochronological data from Anatolia (Table S5). The Tables are stored in the Mendeley Data Base and can be retrieved at <https://data.mendeley.com/datasets/27jpg8z52d/1>.

The ages of the last Cenozoic marine deposits in Anatolia, shown in Figure 2 and Table S1, are obtained mainly from publications with precise biostratigraphic data, preferentially from single individual localities complemented by few chronological ages. The numbers in Figure 2 are linked to Table S1, which includes 216 biostratigraphic localities derived from 157 publications, for each locality, there is information on the respective formation, age, and related reference; the few discrepant ages are discussed at the end of Table S1. The publications used in compiling Table S1 are given in the supplemental references list.

The second set of data, shown in Figures 3 and 4, and given in Table S2, are the ages of the continental Neogene sequences in Turkey based largely on vertebrate studies. This table is an updated version of the compilation by Saraç (2003). Table S2 lists the ages in terms of mammal zones, localities, geographic coordinates, environment of

deposition, and related references (<https://data.mendeley.com/datasets/27jpg8z52d/1>). In some cases, the mammal ages are less precise and extend over a range of mammal zones. In such cases, the mammal ages were distributed evenly to individual mammal zones, as explained in Table S3. The publications used in compiling Table S2 are given in the supplemental references list.

The third data set, shown in Figure 5 and in Table S4, includes the isotopic crystallization ages of the Cenozoic magmatic rocks in Turkey. Table S4 is an updated version of the magmatic age compilations of Türkecan (2015), Ersoy et al. (2017), and Schleiffarth et al. (2018). It includes the method of dating, rock type, locality, and related reference, as well as the numeric ages. The publications used in compiling Table S4 are given in the supplemental references list.

The fourth data set, summarized in Figure 6 and given in Table S5, contains thermochronological ages from Turkey. Table S5 includes the method of dating, numerical age, rock type, locality, and related references (<https://data.mendeley.com/datasets/27jpg8z52d/1>). The ages, which were thought to reflect depositional rather than exhumation ages, are also indicated. The publications used in compiling Table S5 are given in the supplemental references list.

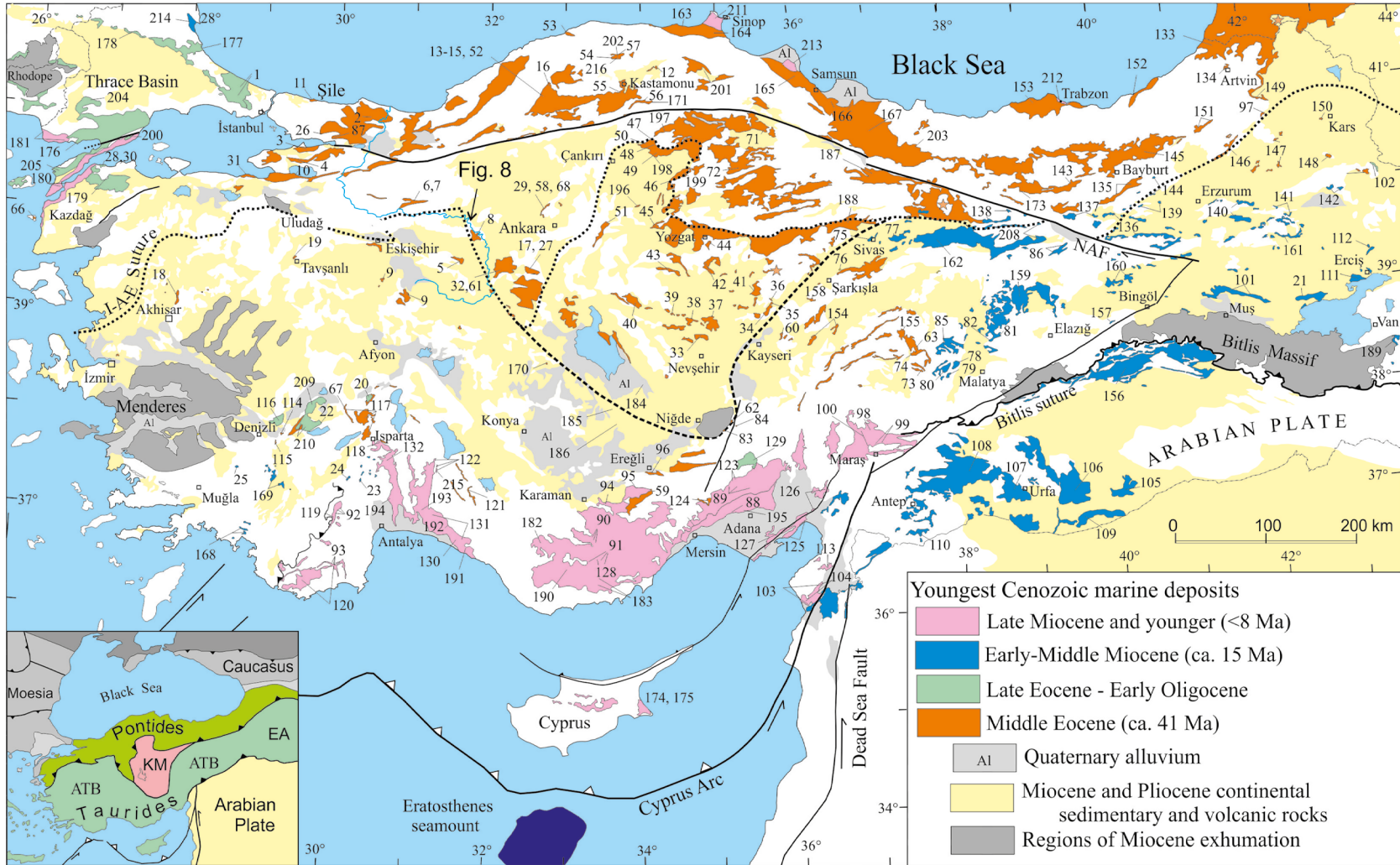


Figure 2. Outcrops of the youngest Cenozoic marine deposits in Anatolia based on the geological map of Turkey (Maden Tetkik ve Arama Genel Müdürlüğü, 2011). The numbers on the map are linked to Table S1. ATB: Anatolide-Tauride Block, KM: Kırşehir Massif, EA: Eastern Anatolia, I-A-E Suture: İzmir-Ankara-Erzincan Suture, NAF: North Anatolian Fault.

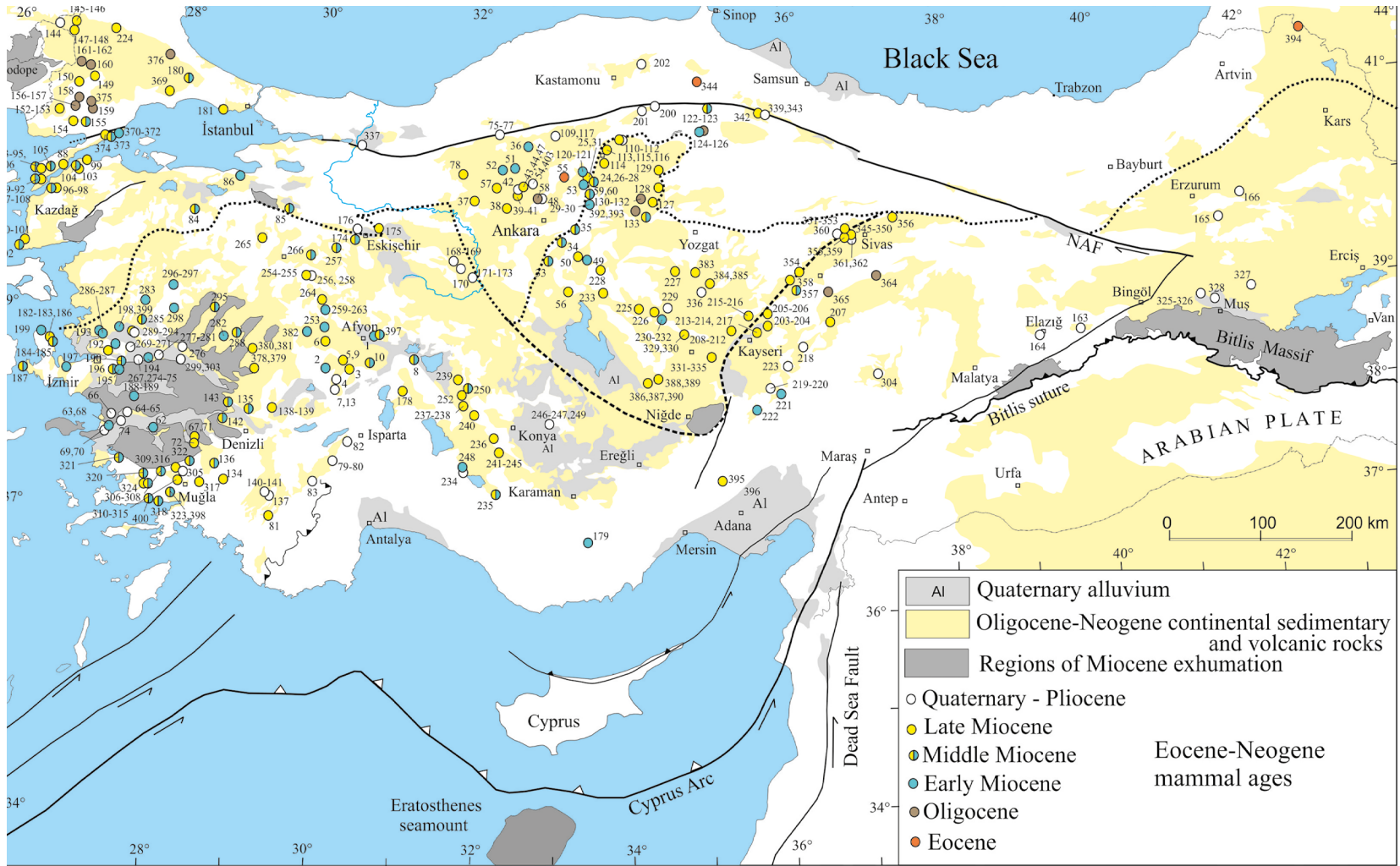


Figure 3. Outcrops of the continental Neogene deposits of Anatolia with locations of the Cenozoic mammal ages. Each locality is numbered and the numbers are linked to Table S2.

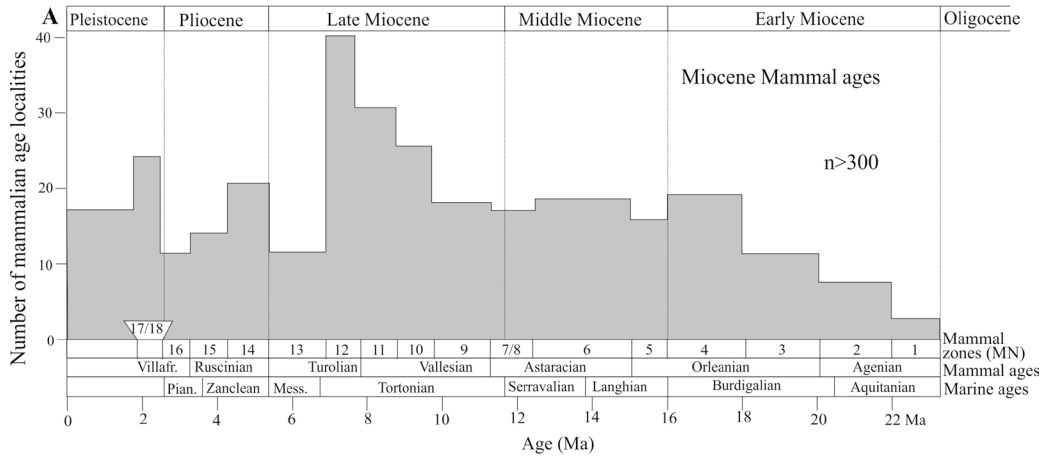


Figure 4. Age-frequency plot of the Cenozoic mammalian ages from Anatolia. For data see Table S2 and Figure 3.

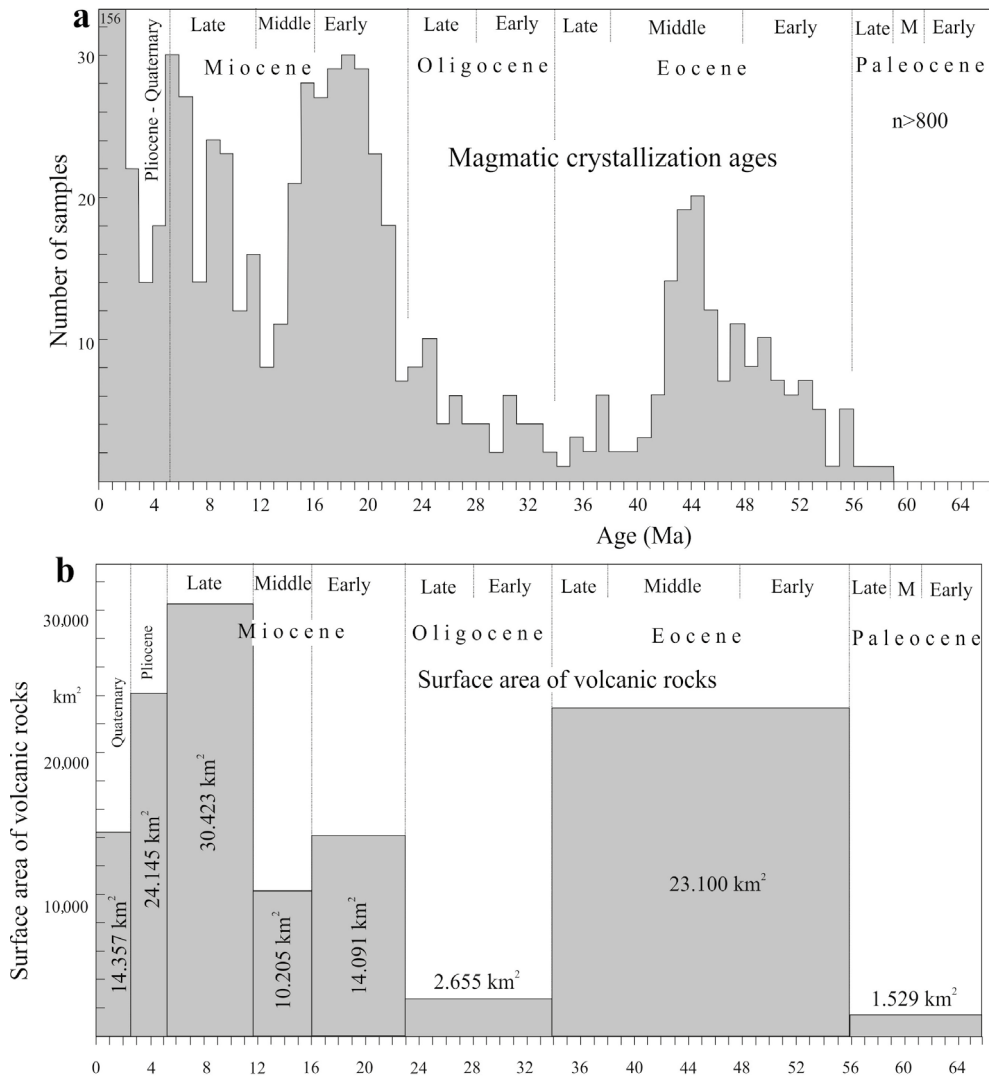


Figure 5. a) Age-frequency plot of the crystallization ages of Cenozoic magmatic rocks from Anatolia. b) Surface area of the Cenozoic magmatic rocks of Turkey (modified from Türkecan, 2015). For data underlying plot (a) see Tables S2 and S3.

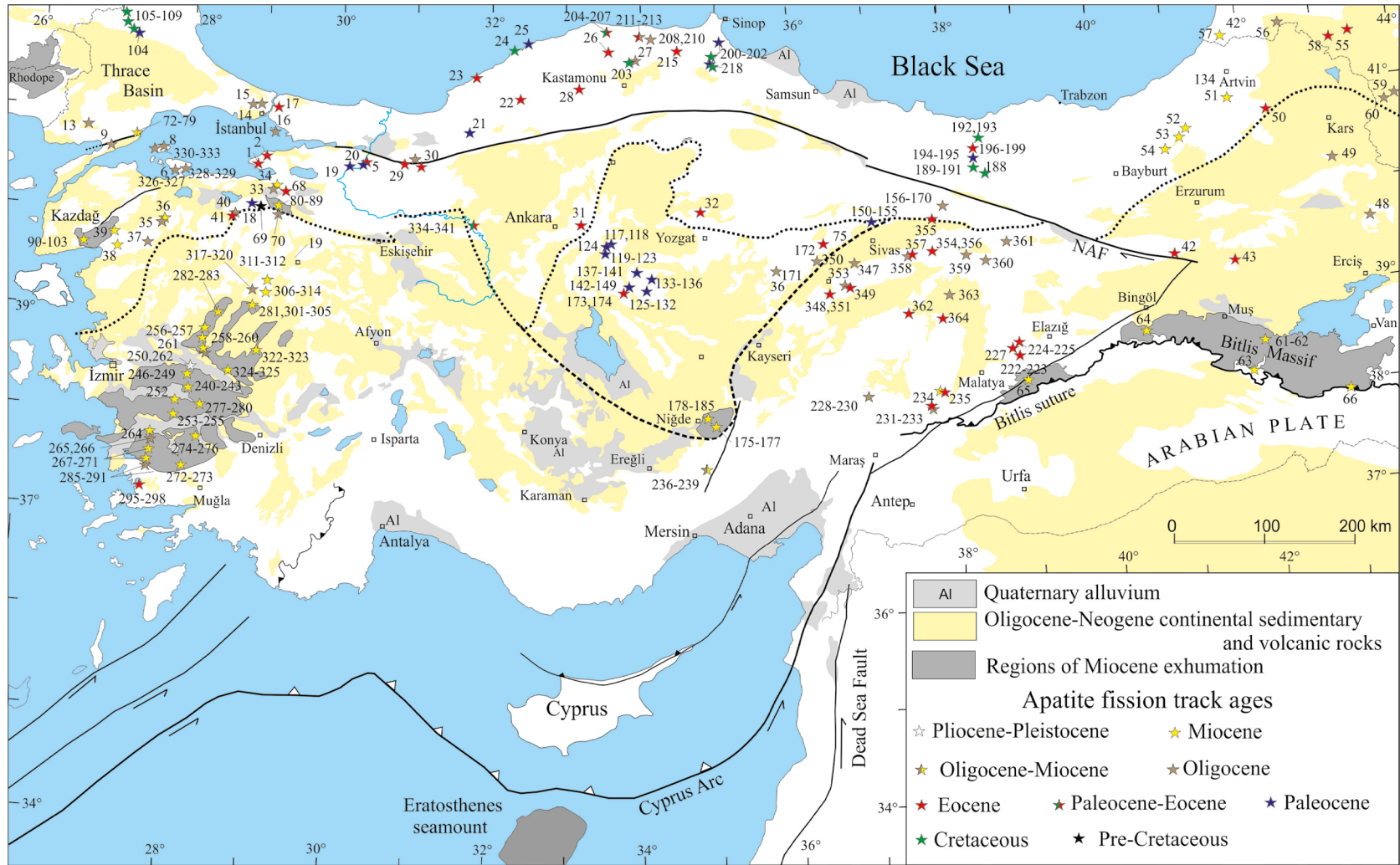


Figure 6. Outcrops of the continental Neogene deposits of Anatolia with locations of published AFT ages. The numbers on the AFT localities are linked to data sources in Table S5.

2.2. Mineral separation, apatite fission track and (U-Th)/He analysis

For the new thermochronological data, reported here, apatite concentrates were separated from samples at the İstanbul Technical University by crushing (jaw crusher), sieving, rinsing and cleaning of samples in water and acetone, magnetic (Frantz magnetic separator) and heavy liquid (sodium polytungstate) separation. Final selection of the apatite grains was achieved by hand-picking under a binocular stereographic microscope.

Apatite grains were mounted in epoxy resin, ground, and polished to expose planar surfaces within the grains and then etched with 5NHNO₃ at 20 °C for 20 s to reveal the spontaneous tracks. The samples were then irradiated with thermal neutrons in the reactor of the Radiation Center at the Oregon State University with a nominal neutron fluence of 9×10^{15} n cm². The standard glass CN-5 was used as a dosimeter to measure the neutron fluence. After irradiation, induced fission tracks (FTs) in the low-U muscovite that covered the apatite grain mounts and glass dosimeter were etched in 40% HF at 20°C for 45 min. Apatite FT(AFT) ages were measured and calculated using the external-detector and zeta-calibration methods with International Union of Geological Sciences (IUGS) age standards (Durango, Fish Canyon and Mount Dromedary apatites) and a value of 0.5 for the $4\pi/2\pi$ geometry correction factor.

Age data are reported as central ages, a weighted modal age calculated through an iterative algorithm. The analyses were subjected to the χ^2 test (Gailbraith, 1981) to detect whether the data sets contained any extra-Poissonian error. A probability of less than 5% denoted a significant spread of single-grain dates.

The apatite concentrates were carefully examined under a stereoscope equipped with a videocamera under transmitted and reflected light in order to select crystals suitable for the (U-Th)/He analysis. The grains should have a section >60 μm , euhedral shape, with no fractures parallel to the c axis, no inclusions, and no coating. Where possible, 3 crystals were selected per single sample. After measurement of their dimensions, the crystals were placed in 0.8-mm-thick Nb tubes and then analyzed at the Thermochronology Laboratory of the Department of Geosciences of the University of Arizona. Samples are first degassed under vacuum by heating with a Nd-YAG laser. Next, the concentration of ⁴He is determined by ³He isotope dilution and measurement of the ⁴He/³He ratio was performed using a quadrupole mass spectrometer. The U, Th, and Sm concentrations were finally obtained via isotope dilution using an inductively coupled plasma mass spectrometer.

3. Biostratigraphy – the last time Anatolia was under the sea

Sea level provides a clear and datable horizon for the uplift history of a region. Figure 2 shows the outcrops of the youngest Cenozoic marine strata in Anatolia. The ages are based on over 200 localities, which are mostly published biostratigraphic sections, supplemented by geochronological ages and a few well logs. The data sources, linked to the numbers on the map, are given in Table S1 (<https://data.mendeley.com/datasets/27jpg8z52d/1>), which also contain details about the stratigraphic sections, lithologies, and ages, and related references.

The map shows three age categories for the youngest Cenozoic marine deposits; in the Pontides and in central Anatolia, the last marine deposits are Middle Eocene (Lutetian, ca. 41 Ma). With the exception of Thrace, no Late Eocene or younger marine deposits have been confirmed over this large area (Lüttig and Steffens, 1976; Özcan et al., 2020). In eastern Anatolia and on the Arabian Platform, the last marine strata are predominantly Lower Miocene (Burdigalian) limestones with some early Middle Miocene marls (Figure 2, Table S1). The Taurides were uplifted above sea level at the end of the Miocene, and locally in the Pliocene and Pleistocene (e.g., Cosentino et al., 2012; Öğretmen et al., 2018). The stratigraphic data indicate that as a whole, central Anatolia and the Pontides became land after ca. 41 Ma, eastern Anatolia and the Arabian Platform after ca. 15 Ma, and most of the Taurides after 8 Ma.

4. Cenozoic continental sedimentation in Anatolia

Middle Eocene and Oligocene (41–22 Ma) continental sediments occur in restricted areas on the Anatolian Plateau, whereas Miocene and younger continental deposits and associated volcanic rocks crop out over extensive areas (Figure 3, Maden Tetkik ve Arama Genel Müdürlüğü, 2011). The Neogene sediments consist mainly of clastic and carbonate rocks and were deposited in fluvial and limnic environments, and in alluvial fans (e.g., Becker-Platen et al., 1977; Arıkan, 1975; Çemen et al., 1999; Gürbüz et al., 2019). The Neogene sequences contain major lignite, borate, and other evaporate deposits and have thicknesses locally exceeding several kilometers (e.g., Kaymakçı et al., 2009; Fernandez-Blanco et al., 2013); individual formations cannot generally be traced more than a few tens of kilometers, as they were deposited in isolated lakes with shifting boundaries and in local fluvial systems. This represents a problem in establishing the precise ages of the Neogene sedimentation in Anatolia. One proxy in this respect is the distribution of the mammal ages. Mammal fossils provide precise and accurate ages, and are

calibrated into mammal zones (e.g., Steininger et al., 1996). A compilation of Cenozoic mammal ages in Anatolia was provided by Saraç (2003); this compilation was updated herein, in Table S2, which includes the geographic coordinates, depositional environment, and related references of over 400 individual mammal age localities (<https://data.mendeley.com/datasets/27jpg8z52d/1>). Their distribution is shown on the map in Figure 3. Each mammal locality in Figure 3 is linked to Table S2 through numbering. Figure 3 illustrates the wide distribution of Early, Middle, and Late Miocene and Pliocene mammal localities in western and central Anatolia. This is also displayed in the age-frequency diagram in Figure 4, which indicates a relatively even distribution of mammal ages from the Miocene to Recent, except for a dearth of earliest Miocene and a relative concentration of Late Miocene mammal ages. The distribution of the mammal ages suggest that continental sedimentation in western and central Anatolia took place semicontinuously from the Early Miocene to the present (e.g., Alçiçek, 2010).

The Miocene sediments on the Anatolian Plateau were deposited either in extensional tectonic environments, as shown by the presence of Miocene metamorphic core complexes, such as the Kazdağ and Menderes massifs, or in contractional settings, such as those in the Çankırı Basın (Kaymakçı et al., 2009). They are generally less than one kilometer thick, although in individual basins may be several kilometers. Despite variations in the tectonic setting and thickness of the Miocene and younger sediments, and despite Miocene global sea level fluctuations of more than 150 m (e.g., Haq et al., 1987), the Miocene and younger sequences of central Anatolia contain no marine intercalations and the shoreline was relatively constant, closely following the northern boundary of the Tauride mountain chain (Figure 2). This indicates that the surface uplift kept pace with subsidence during the Miocene and later.

5. Cenozoic magmatism in the Anatolian Plateau

Neogene volcanic rocks cover large areas on the Anatolian Plateau (Türkecan, 2015), whereas they are virtually absent in the Taurides and are rare in the Pontides. Recent compilations of Cenozoic crystallization ages of the Anatolian magmatic rocks by Türkecan (2015), Ersoy et al. (2017), and Schleiffarth et al. (2018) have been merged and updated in Table S4 (<https://data.mendeley.com/datasets/27jpg8z52d/1>). The age-frequency histogram in Figure 5a indicate a magmatic quiescence in the Paleocene followed by a magmatic peak in the Middle Eocene. A similar picture emerges from the surface area distribution of the Cenozoic volcanic rocks in Turkey (Figure 5b; Türkecan, 2015).

The bulk of the volcanism in the Middle Eocene was submarine and associated with marine sedimentation,

and corresponds to a postcollisional extensional phase. The Middle Eocene magmatism was followed by a second quiet period in the Late Eocene and Oligocene (Figure 5); a surge in continental volcanism starts in the Early Miocene (ca. 22 Ma) and continues to the present (e.g., Innocenti et al., 2005; Dilek and Altunkaynak, 2009; Sarıkaya et al. 2019). This was also the period of extensive continental sedimentation on the Anatolian Plateau (Figure 2).

6. Thermochronology – exhumation of the Central Anatolian Plateau

The distribution of marine strata in Anatolia indicate that it became land after the early Middle Eocene (Lutetian); therefore, any exhumation of the Anatolian landmass must have occurred after 41 Ma. Thermochronological data from Anatolia have been compiled in Table S5 and the apatite fission track (AFT) ages are shown in Figure 6, which are linked to Table S5 through numbering. The AFT data show three distinct age peaks at the Middle-Late Paleocene, Oligocene, and Miocene; pre-Cenozoic ages make up less than 7% of the total. The Miocene exhumation was focused on isolated metamorphic core complexes, such as the Menderes and Kazdağ massifs in western Anatolia (Ring et al., 2003; Cavazza et al., 2009) or the crystalline thrust wedges, such as the Bitlis Massif (Okay et al., 2010). The prominent Miocene peak reflects the high concentration of AFT samples from the Miocene metamorphic core complexes (Figure 7); however, regions with rapid Miocene exhumation make up less than one-tenth of the surface area of Anatolia. The Paleocene-Eocene AFT ages come mainly from central Anatolia and the Pontides (Figure 6, Table S5), and are related to exhumation following the collision between the Pontides and the Anatolide-Tauride Block/Kırşehir Massif. The Oligocene AFT ages (30–27 Ma) come from a large area (Figure 6) and correspond to an exhumation phase prior to the widespread Miocene continental sedimentation.

With the exception of the Kırşehir Massif, data on the exhumation of central Anatolia are rare. This is mainly due to minor late Cenozoic erosion and minor relief of the Central Anatolian Plateau, which makes quantifying the Cenozoic exhumation difficult. An ideal place to date the exhumation would be a deeply incised valley not related to a late Cenozoic structure. Such a region is provided by the Sakarya Valley in central Anatolia (Figure 8). The 824-km-long Sakarya River originates in central Anatolia and flows into the Black Sea. West of Ankara, it forms a 1000-m-deep valley with a 500-m-deep inner canyon (Figures 8 and 9). The Sakarya Canyon cuts through a Late Cretaceous pluton, the Beypazarı Granite. The incision is controlled by the base level of the Black Sea and is not related to a particular structure.

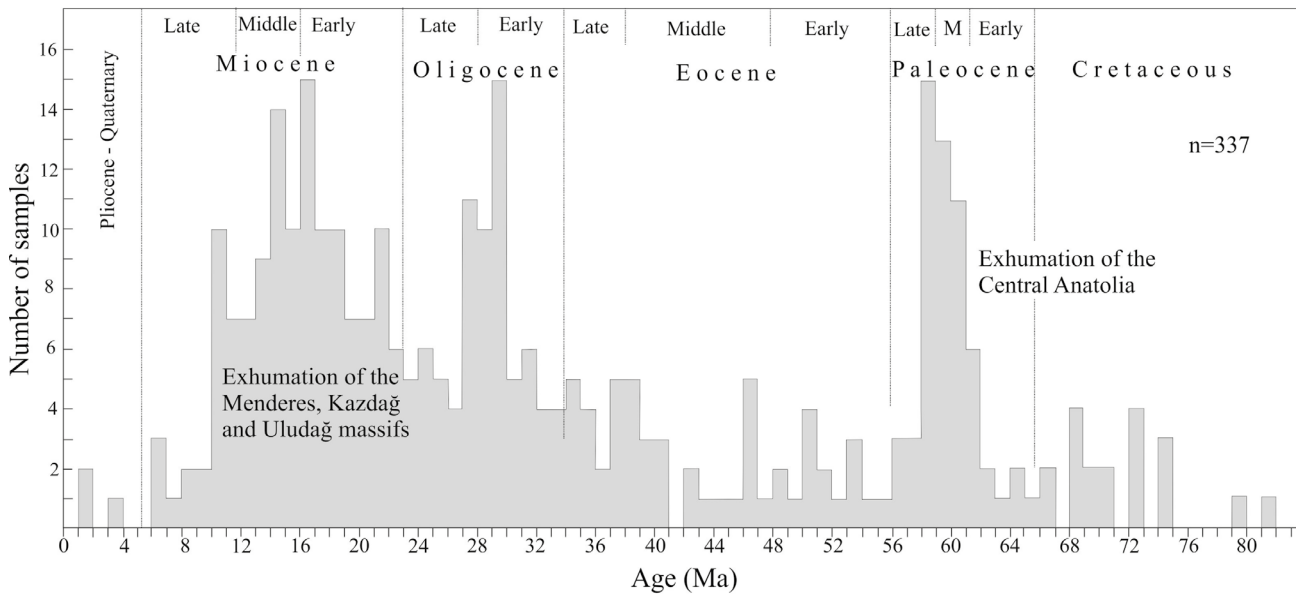


Figure 7. Age-frequency plot of AFT exhumation ages from the Anatolia. For data see Figure 6 and Table S5.

The Beypazarı Granite is a coarse-grained granodiorite of quartz, plagioclase, K-feldspar, biotite, and hornblende (Öztürk et al., 2012). Zircon U-Pb ages from the Beypazarı Granite are 74.0 ± 1.0 Ma (Helvacı et al., 2014; Okay et al., 2019, 2020) and indicate crystallization in the Late Cretaceous. The Beypazarı Granite intrudes into metamorphic rocks (Figure 8). In the north, this contact is overprinted by a transpressive shear zone (Okay et al., 2020). In the south, the Beypazarı Granite is unconformably overlain by a 500-m-thick Eocene sequence of fluvial sandstone, mudstone, and minor conglomerate, with horizons of shallow marine sandy limestone (Figures 8 and 9d). The first marine strata, with a rich fauna of large benthic foraminifera, are found ~60 m above the granite. The foraminifera included *Alveolina kieli*, *Alveolina tenuis*, *Alveolina cf. delicatissima*, *Alveolina orhaniyensis*, *Discocyclina radians*, *Discocyclina fortisi*, *Discocyclina dispansa*, and *Nemkovella* sp. (Figure 10) and indicate an early Middle Eocene [early Lutetian, shallow benthic zone (SBZ) 13] age. Thus by 48–45 Ma, the Beypazarı Granite was exposed to near sea level. The Middle Eocene marine transgression documented over the Beypazarı Granite is widespread in central Anatolia (Figure 2).

A Neogene lacustrine marl sequence, several hundreds of meters thick, covers unconformably the older units along a subhorizontal erosion surface at an elevation of ~1000 m. (Figures 8, 9b, and 9c). This surface is close to the mean elevation of the Central Anatolian Plateau (~1 km). The Neogene sequence is likely to be of Early Pliocene age based on vertebrate fossils from neighboring regions (Şen et al., 2017).

To date the exhumation of the Beypazarı Granite, samples were collected from a vertical profile along the Sakarya Valley for the AFT and apatite (U-Th)/He (AHe) analyses (Figure 8). The AFT results show an age range from 72 to 47 Ma (Table, Figure 11), suggesting that cooling through the apatite fission-track closure temperature took place mainly in the Paleocene-Early Eocene, which is compatible with the unconformable Middle Eocene strata. Cooling to lower temperatures is recorded by AHe data, which are, within errors, younger than the AFT data, as expected; they span from the Eocene to Early Miocene (Figure 11, Table). The AHe data show a good correlation between age and elevation for the samples collected along the vertical profile. The AHe age of the highest-elevation sample (8821, 45 Ma) is similar to the age of the Eocene marine transgression (48–45 Ma, Figure 11), indicating that the sample was not exhumed or buried significantly (< 2 km) since the Middle Eocene. Two samples collected close to the shear zone north of the vertical profile (samples 9450 and 9456) produced the oldest AHe ages, pointing to some tectonic disturbance on the distribution of ages (Table).

HeFTy software (Ketcham, 2005) was used to generate a range of possible T-t paths using a Monte-Carlo algorithm. Inversion models for different samples are remarkably similar, showing a main exhumation event in the Late Cretaceous-Early Paleocene, followed by a long period of relative stability until the present day (Figure 12). During this latter period, the granites were buried by some hundreds of meters of sediments and then exhumed again to the surface. However, the thermochronometric systems

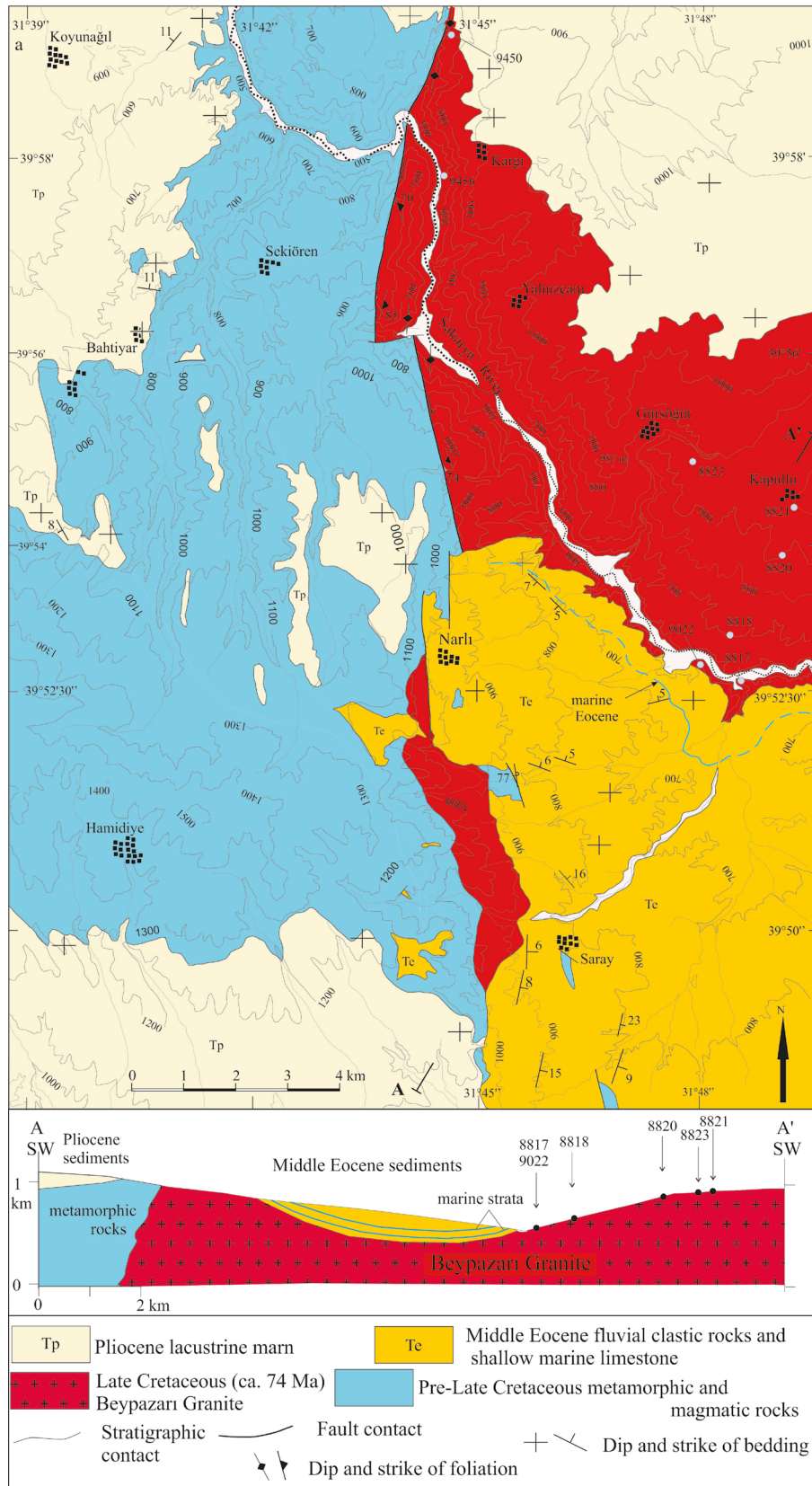


Figure 8. Geological map and cross-section of the Sakarya Canyon west of Ankara, for location see Figure 2.

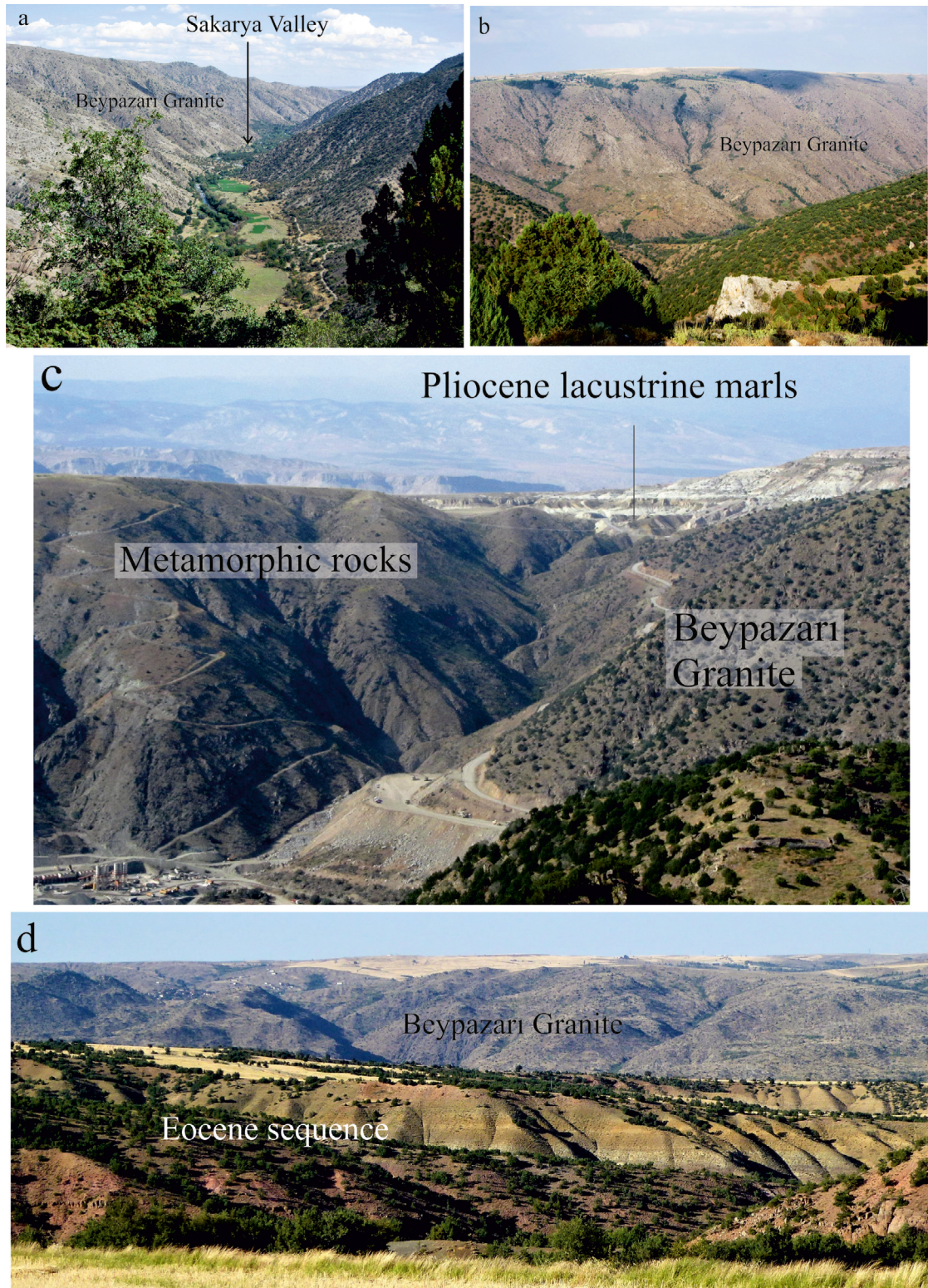


Figure 9. Field photographs of the Beypazari Granite, Central Anatolia. a) Sakarya Valley looking south. b) The eastern flank of the Sakarya Valley, where the thermochronological samples are collected. The flat surface at the top at a height of ca. 1000 m represents an erosion surface, similar to the elevation of the Central Anatolian Plateau. c) The onlap of Pliocene lacustrine sediments on the Beypazari Granite and the metamorphic rocks. d) The Eocene sequence and the Beypazari Granite.

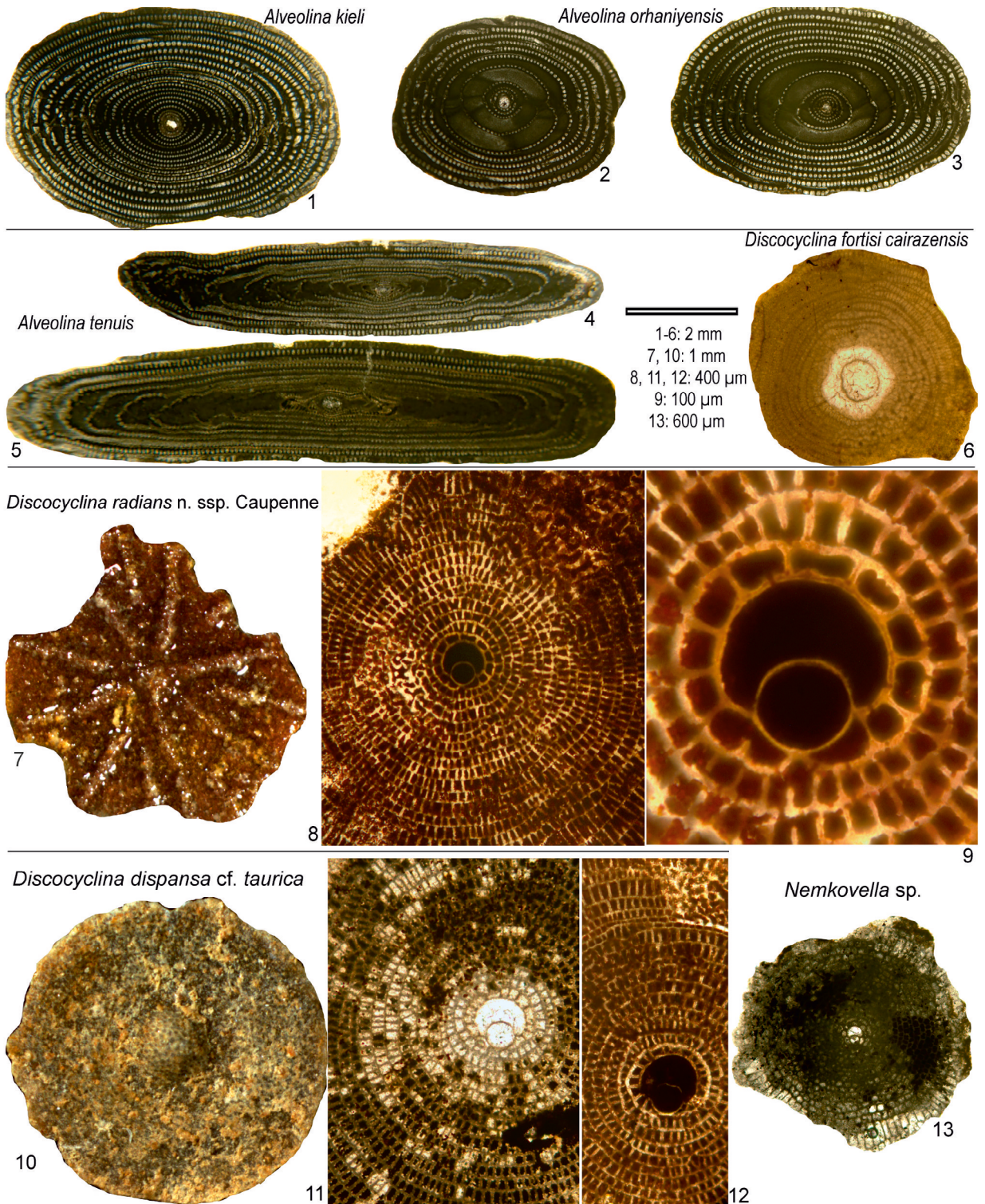


Figure 10. Larger benthic foraminifera (alveolinids and orthophragminids) from the Lower Lutetian transgressive sequence overlying the Beypazarı granite. 1) Sample 8814-1, 2) sample 8814-2, 3) sample 8814-3, 4) sample 9026-1, 5) sample 9026-4, 6) sample 9029-2, 7) sample 9031-12, 8-9) sample 9029-1, 10-11) sample 9031-3, 12) sample 9031-13, 13) sample 9031-25.1-5) axial sections; 6, 8-9, 11-13) equatorial sections; 7, 10) external views.

Table. Thermochronological data from the Beypazari Granite in the Sakarya River Valley.

APATITE U-Th/He DATA																
Grain No.	Raw age (Ma)	$\pm\sigma$ (Ma)	Radius (μm)	U (ppm)	Th (ppm)	Sm (ppm)	4He (nmol/g)	eU (ppm)	FT 238U	FT 235U	FT 232Th	FT 147Sm	Fully FT corr. age (Ma)	$\pm\sigma$ (Ma)	Weighted mean age (Ma)	$\pm\sigma$ (Ma)
8817_1	4.36	0.64	49.64	49.86	107.9	14.34	1.77	75.21	0.71	0.68	0.68	0.92	6.22	0.92		
8817_2	12.47	0.24	66.91	21.63	43.89	137.07	2.17	31.95	0.78	0.75	0.75	0.93	16.11	0.31	18.91	0.27
8817_3	32.88	0.56	52.71	17.71	38	134.84	4.77	26.64	0.73	0.69	0.69	0.91	45.75	0.78		
8818_2	26.35	0.58	57.22	16.69	43.34	287.77	3.89	26.88	0.75	0.71	0.71	0.92	35.68	0.79		
8818_3	19.8	0.43	62.72	18.98	50.36	260.06	3.34	30.81	0.77	0.74	0.74	0.93	26.9	0.57	30.62	0.4
8818_4	22.91	0.55	49.57	18.02	46.11	301.58	3.62	28.85	0.71	0.68	0.68	0.91	32.64	0.78		
8820_1	25.74	0.55	68.48	18.72	51.01	337.01	4.34	30.7	0.79	0.76	0.76	0.93	33.06	0.71		
8820_2	35.36	0.77	67.53	18.87	51.08	371.74	6	30.88	0.78	0.76	0.76	0.93	45.58	1	37.33	0.47
8820_3	27.03	0.6	53.46	22.89	60.91	366.13	5.51	37.2	0.73	0.7	0.7	0.91	37.48	0.83		
8821_1	30.53	0.87	74.04	26.22	67.51	228.2	7.01	42.08	0.8	0.78	0.78	0.94	38.48	1.1	45.09	0.81
8821_3	36.45	0.83	47.11	23.44	63.88	237.25	7.65	38.46	0.7	0.66	0.66	0.9	53.09	1.21		
9022_1	20.42	0.45	55.34	19.69	45.99	168.3	3.39	30.5	0.74	0.71	0.71	0.92	27.97	0.62		
9022_2	18.17	0.41	63.7	18.16	42.12	153.33	2.78	28.06	0.77	0.74	0.74	0.93	23.82	0.53	22.91	0.28
9022_3	14.02	0.26	46.19	22.6	48.47	146.29	2.59	33.99	0.69	0.65	0.65	0.9	20.55	0.38		
9450_2	40.38	0.71	57.62	24.29	52.15	201.52	8.05	36.55	0.75	0.72	0.72	0.92	54.5	0.96	55.25	0.68
9450_3	43.29	0.74	66.32	25.1	53.22	225.47	8.89	37.61	0.78	0.75	0.75	0.93	56.02	0.97		
9456_1	36.35	0.45	61.67	20.67	41.93	127.18	6.04	30.53	0.77	0.73	0.73	0.93	48.04	0.83		
9456_2	41.78	0.41	84.54	22.03	48.14	144.84	7.59	33.34	0.83	0.8	0.8	0.94	51.04	0.87	47.5	0.47
9456_3	33.1	0.26	59.07	24.82	50.59	120.43	6.61	36.71	0.76	0.72	0.72	0.92	44.35	0.76		

Raw age ($\pm\sigma$): Age of the grain before the correction. U, Th, Sm (ppm): U, Th, and Sm contents.

4He (nmol/g): Concentration of He measured by the mass spectrometer.

eU (ppm): Effective Uranium, quantity typically used to represent the concentration of U and Th. It is calculated according to the formula: $eU = [U] + 0.235 \times [Th]$. In Table 1, data for grains with $eU < 5$ ppm are represented in italic font.

FT 238U, 235U, 232Th, 147Sm: Alpha-ejection correction factor. The resulting dates require a correction for He loss occurred by the ejection of α particles outside of the crystal domain. Moreover, since the α particles emitted by U, Th, and Sm travel a distance of ca. 20 μm , part of those emitted close to the crystal edges are ejected out of the crystal. The loss of α particles leads to an underestimation of the age of the crystal. The magnitude of α -ejection is controlled by the surface to volume ratio and by spatial distribution of the parent atoms relative to the crystal surface. Assuming an idealized geometry of the crystal and a homogeneous distribution of U, Th, and Sm in the crystal, the fraction of He retained can be calculated as a function of the crystal size, as described by Farley (2002). Therefore, to account for α -ejection it is a common practice to measure the physical dimensions of the crystal to be dated and to calculate a homogeneous α -ejection correction factor, to which the raw date has to be multiplied, to obtain the age corrected for ejection (Farley, 2002).

Fully corrected FT age ($\pm\sigma$): Age of the grain after the correction.

Table. (Continued).

Table. Thermochronological data from the Beypazari Granite in the Sakarya River Valley.

Sample No.	No. of crystals	Spontaneous		Induced		$P(c)^2$	Dosimeter		Height m	Age (Ma) $\pm 1s$	Mean confined track length (mm) \pm standard error	Standard deviation	No. of tracks measured
		r_s	N_s	r_i	N_i		r_d	N_d					
TU8817	20	5.32	619	1.56	1812	52.0	1.19	5870	587	69.8 \pm 5.1	13.44 \pm 0.14	1.11	62
TU9022	20	4.64	476	1.45	1493	97.5	1.17	5836	596	64.1 \pm 4.9	13.15 \pm 0.12	1.16	100
TU8818	20	5.05	603	1.46	1741	40.5	1.21	5902	697	72.0 \pm 5.3	13.38 \pm 0.11	1.09	100
TU8820	20	4.63	334	1.57	1129	74.5	1.20	5880	893	61.0 \pm 5.1	13.94 \pm 0.12	1.14	95
TU8823	20	4.35	476	1.64	1795	60.0	1.19	5858	958	54.3 \pm 4.1	13.73 \pm 0.12	1.12	92
TU8821	20	7.12	656	2.20	2028	28.7	1.21	5892	986	66.8 \pm 5.0	14.10 \pm 0.10	0.92	95
TU9456	20	4.14	462	1.72	1917	69.6	1.13	5758	511	46.9 \pm 3.6	13.48 \pm 0.08	0.86	100
TU9450	20	4.89	511	1.59	1665	18.0	1.14	5770		60.0 \pm 4.7	n.d.	n.d.	n.d.

Central ages were calculated using dosimeter glass CN5 and ζ -CN5 = 345.53 \pm 18.45.

* ρ_s : Spontaneous track densities ($\times 105 \text{ cm}^2$) measured in internal mineral surfaces.

† N_s : Total number of spontaneous tracks. ρ_i and ρ_d : Induced and dosimeter track densities ($\times 106 \text{ cm}^2$) on external mica detectors ($g = 0.5$).

N_i and N_d : Total numbers of tracks.

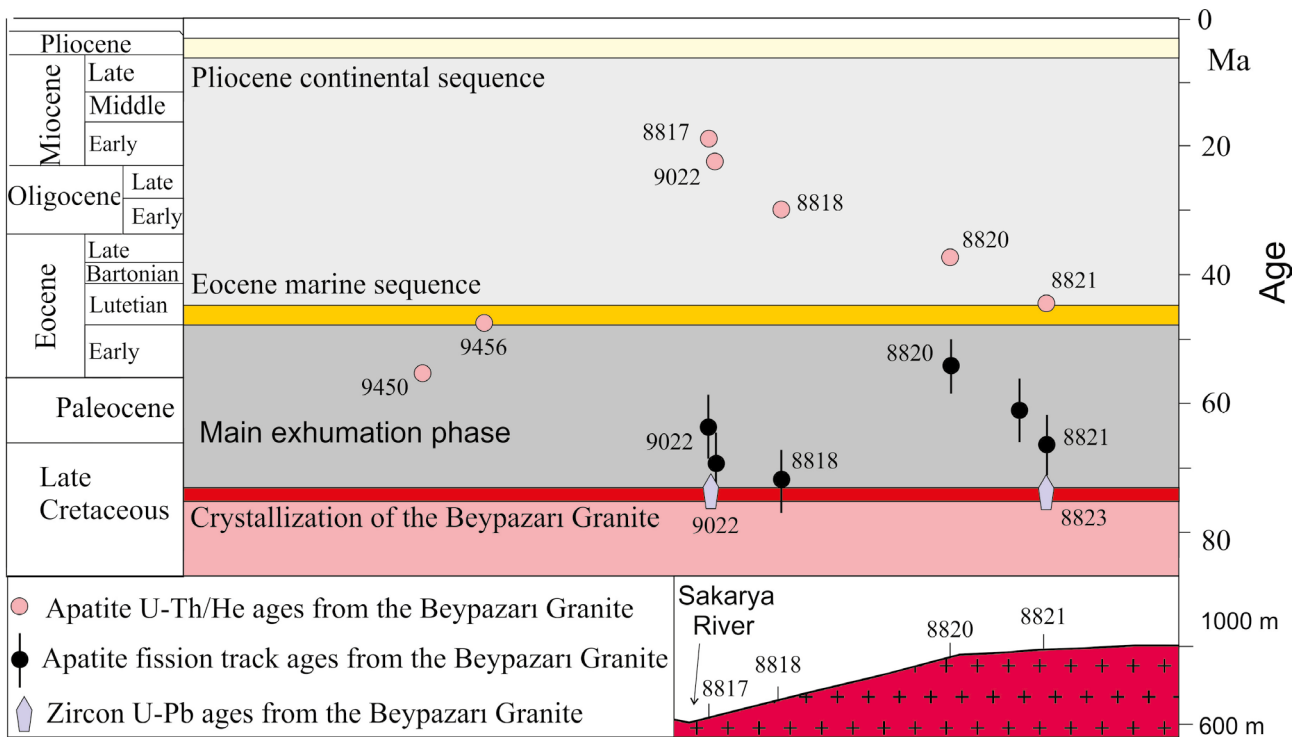


Figure 11. Thermochronological data plotted against time. The inset shows the topography and some of the sample locations. Sample locations are also shown in the geological map in Figure 8.

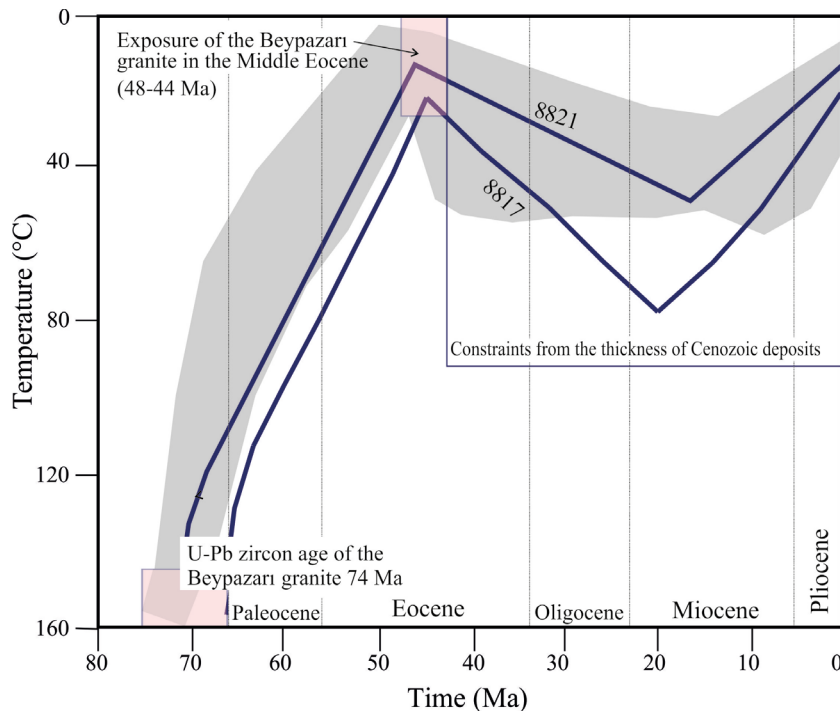


Figure 12. Time-temperature paths obtained from inverse modeling of apatite fission-track data. The Figure shows the complete results for sample 8821 as reference and best results for sample 8817. Grey area marks envelopes of statistically acceptable fit, and the thicker lines correspond to the weighted mean path. Boxes represent T-t domains constrained by available data.

used are not sensitive to temperatures lower than 50 °C; thus, it is not possible to place a solid constraint on the time and temperature of maximum burial. The highest values of the burial temperatures are detected on sample 8817 and are in the order of 80 °C, while the lowest values (50–60 °C) are derived from modeling of sample 8821 (Figure 12). The different AHe ages that are read along the profile are thus, not related to slow and steady-state exhumation, but to the increase of burial from the top to the bottom of the profile. In other words, the sample on top was older because it had not been reset at all. This means that: i) maximum burial was attained when the relative position between samples was the same as today, i.e. no major tilting or differential vertical displacement took place since burial; and ii) the linear age-elevation relationships detected on AHe data could not be interpreted as the signature of en bloc exhumation of the granite. The regression line, therefore, could not be used to estimate the exhumation rate. Overall the AHe thermochronology ages indicate a period of relative stability since 45 Ma, with slow exhumation/subsidence rates (<0.07 km/Myr).

The spatial relation between the Pliocene lacustrine sediments and the Sakarya Canyon indicate that the

canyon was carved after the deposition of the Cenozoic sediments (Figure 9c). Potentially, this provides a rate for river incision and indirectly for rock uplift. Two uncertainties are the age of the lacustrine sediments and the sea level of the Black Sea during incision. In the Kazan region, about 80 km east-northeast of Beypazari, the continental Cenozoic sediments have been dated as Early Pliocene (MN14, ca. 5 Ma, Sen et al., 2017). At 5 Ma, the sea level in the Black Sea was close to the present (e.g., Tari et al., 2019). These values indicated 500 m of incision in the last 5 million years, giving an average incision value of 0.05 mm/y, similar to that obtained from the thermochronology.

7. Discussion and conclusions

The biostratigraphy shows that the last marine strata in central Anatolia and the Pontides are of Middle Eocene age (ca. 41 Ma). The absence of post-Middle Eocene marine sediments on the Anatolia Plateau is a primary feature rather than that of preservation or recognition, as shown by the continental nature of the post-Middle Eocene sediments. Furthermore, post-Middle Eocene marine sediments, if they were deposited, would have been at least

locally preserved under the extensive Neogene continental sedimentary cover (Figure 2), especially considering that erosion has not been significant uniformly across Anatolia since 41 Ma. However, this is not the case; therefore, it is concluded that the Anatolian Plateau has stayed above sea level since 41 Ma.

The post-Middle Eocene history of the Anatolian Plateau can be considered in two stages. During the Late Middle Eocene and Oligocene (41–22 Ma), there was local continental deposition, local exhumation, and minor magmatism (Figure 3), which were followed by extensive continental sedimentation and associated magmatism in the Miocene and later. The latter was also the period of extensional exhumation of metamorphic core complexes, such as the Menderes and Kazdağ massifs (Ring et al., 2003; Cavazza et al., 2009). Although there was local subsidence during the Neogene, the Anatolian Plateau region stayed above sea level, which indicates that regional rock uplift was higher than local subsidence.

We propose that the depositional environment and topography of central Anatolia has changed little since the Late Middle Eocene (ca. 41 Ma, Lutetian), and particularly since the Early Miocene (ca. 22 Ma). This is based on the following data and observations.

a) Despite local subsidence and sea level variations in the last 22 Ma, central and western Anatolia have continued to be a land area with a relatively constant coastline following the northern boundary of the Taurides (Figure 2), indicating a relief of at least several hundred meters.

b) The thickness of the Eocene and Miocene marine deposits is generally less than 500 m (Table S1). Their widespread preservation shows that, with some notable exceptions, such as the Menderes Massif, erosion has not been significant in Anatolia (>1 km) since the Middle Eocene, which is corroborated by the thermochronological data.

c) The mammal ages imply semicontinuous continental sedimentation from the Early Miocene to present (Figure 3).

d) The areas of current sedimentation on the Anatolian Plateau, such as Salt Lake in central Turkey, and many alluvial plains, are generally located within large Neogene outcrops (Figure 2), indicating that in many regions, Miocene depositional and tectonic patterns are continuing today.

e) Neogene basins in Anatolia occupy generally low-lying flat topography surrounded by basement outcrops forming the hills, indicating a continuing pattern of sedimentation.

f) Early Miocene continental magmatism has continued without significant interruption to the present.

g) Miocene metamorphic core complexes, such as the Menderes and Kazdağ massifs, form mountains and are

associated with active extensional to transtensional faults (e.g., Baran et al., 2017; Cavazza et al., 2009; Okay et al., 2008).

The widespread preservation of Eocene deposits and extensive Neogene outcrops indicate that, with some exceptions, erosion or subsidence on the Anatolian Plateau has generally not exceeded one kilometer since 41 Ma. Modeling of several deep hydrocarbon wells in the Salt Lake Basin in central Anatolia indicate less than 500 m of burial or erosion since 41 Ma (Huvaz, 2009). Considering that the Anatolian Plateau has been above sea level since 41 Ma, the long-term surface uplift/subsidence rates in this period were in the order of 0.02–0.03 km/Myr.

The uniform pattern of sedimentation and volcanism of the Anatolian Plateau since 22 Ma is in contrast with the Cenozoic story of its southern margin, the Taurides. The Taurides is largely free of Neogene magmatism and rose above sea level in the Late Miocene (8 Ma), when it underwent a fast uplift (0.2–0.4 km/Myr, Cosentino et al., 2012; Schildgen et al., 2014). Recent data have indicated that in the last 0.6 Ma, the uplift rate has increased to over 1 km/Myr (Öğretmen et al., 2018). There are a few data on the uplift rate of the Eastern Anatolian Highlands; however, its present elevation of 2 km and widespread distribution of Lower-Middle Miocene (15 Ma) marine sediments suggest uplift rates comparable with those of the Taurides (0.1–0.2 km/Myr). The only effect of the recent fast uplift of the Taurides on the Anatolian Plateau appear to be an increase in magmatism in the Late Miocene (Figure 5).

The uplift of the Taurides and eastern Anatolia was generally linked to the delamination of the Eastern Mediterranean oceanic lithosphere, followed by slab break-off and asthenospheric upwelling (e.g., Keskin, 2003; Cosentino et al., 2012; Schildgen et al., 2014). The difference between these regions is that in eastern Anatolia, the Mediterranean ocean closed in the Early Miocene through collision between Arabia and Eurasia (Okay et al., 2010), whereas oceanic subduction continued under Anatolia. Bartol and Govers (2014) suggested that the uplift of the Central Anatolian Plateau was related to the westward progression of the East Anatolian lithospheric delamination. Göğüş et al. (2017) invoked drip of the lithospheric mantle was responsible for the uplift of the whole of Anatolian region. Both studies assumed that the uplift has occurred since 10 Ma. However, as shown herein, Anatolia has been in a steady state in terms of tectonic environment over the last 22 million years. It is likely that flat subduction at a low constant rate during the Late Eocene and Oligocene, and mantle upwelling in the Miocene, maintained Anatolia dynamically above sea level (e.g., Faccenna et al., 2013; Govers and Fichtner, 2016).

In conclusion, central Anatolia was uplifted above sea level at ca. 41 Ma, and since ca. 22 Ma has been on a steady state with continental sedimentation and volcanism, with

little change in the surface uplift/subsidence rates (<0.05 km/Myr), except in the Miocene core complexes. This contrasts with the much younger (after 8 Ma) and faster uplift (>0.4 km/Myr) of the Taurides. The uplift of central Anatolia and the Taurides cannot be ascribed to the same cause. The Anatolian Plateau is a composite structure, which grew southward after the Late Miocene.

Acknowledgments

The study was supported by the Scientific and Technological Research Council of Turkey (TÜBİTAK), under grant No.

References

- Alçıçek H (2010). Stratigraphic correlation of the Neogene basins in southwestern Anatolia: regional palaeogeographical, palaeoclimatic and tectonic implications. *Palaeogeography Palaeoclimatology Palaeoecology* 291: 297-318.
- Arıkan Y (1975). The geology and petroleum prospects of the Tuz Gölü Basin. *Bulletin of the Mineral Research and Exploration Institute of Turkey* 85: 17-44.
- Baran ZO, Dilek Y, Stockli D (2017). Diachronous uplift and cooling history of the Menderes core complex, western Anatolia (Turkey), based on new zircon (U-Th)/He ages. *Tectonophysics* 694: 181-196.
- Bartol J, Govers R (2014). A single cause for uplift of the Central and Eastern Anatolian plateau? *Tectonophysics* 637: 116-136.
- Becker-Platen JD, Benda L, Steffens P (1977). Litho- und biostratigraphische Deutung radiometrischer Altersbestimmungun aus dem Jungtertiär der Türkei. *Geologisches Jahrbuch B25*: 139-167.
- Berndt C, Yıldırım C, Çiner A, Strecker M, Ertunç G et al. (2018). Quaternary uplift of the northern margin of the Central Anatolian Plateau: New OSL dates of fluvial and delta-terrace deposits of the Kızılırmak River, Black Sea coast, Turkey. *Quaternary Science Reviews* 201: 446-469.
- Cavazza W, Okay AI, Zattin M (2009). Rapid early-middle Miocene exhumation of the Kazdağ metamorphic core complex (Western Anatolia). *International Journal of Earth Sciences* 98: 1935-1947.
- Çemen İ, Göncüoğlu MC, Dirik K (1999). Structural Evolution of the Tuzgölü Basin in Central Anatolia, Turkey. *Journal of Geology* 107: 693-706.
- Çiner A, Doğan U, Yıldırım C, Akçar N, Ivy-Ochs S et al. (2015). Quaternary uplift rates of the Central Anatolian Plateau, Turkey: insights from cosmogenicisochron-burial nuclide dating of the Kızılırmak River terraces. *Quaternary Science Reviews* 107: 81-97.
- Cosentino D, SchildgenTF, Cipollari P, Faranda C, Gliozzi E et al. (2012). Late Miocene surface uplift of the southern margin of the Central Anatolian Plateau, Central Taurides, Turkey. *Geological Society of America Bulletin* 124: 133-145.
- 113R007, and the Turkish Academy of Sciences (TÜBA). We thank Oğuz Göğüş, Ali Uygun, Evren Çubukçu, and Aynur Hakyemez for discussions and Taylor Schildgen, Attila Çiner, Rob Govers, and several anonymous reviewers for their corrections and suggestions.
- ### Supplemental Tables and Figures
- The tables and references given in the manuscript can be accessed using the following link: <https://data.mendeley.com/datasets/27jpg8z52d/1>
- Dilek Y, Altunkaynak Ş (2009). Geochemical and temporal evolution of Cenozoic magmatism in western Turkey: mantle response to collision, slab break-off, and lithospheric tearing in an orogenic belt. In: Van Hinsbergen DJJ, Edwards MA, Govers R (editors). *Collision and Collapse at the Africa–Arabia–Eurasia Subduction Zone. The Geological Society Special Publication (Book 311)*. London, UK: The Geological Society of London, pp. 213-233.
- Ersoy Y, Akal C, Genç ŞC, Candan O, Palmer MR et al. (2017). U-Pb zircon geochronology of the Paleogene – Neogene volcanism in the NW Anatolia: Its implications for the Late Mesozoic-Cenozoic geodynamic evolution of the Aegean. *Tectonophysics* 717: 284-301.
- Faccenna C, Becker TW, Jolivet L, Keskin M (2013). Mantle convection in the Middle East: Reconciling Afar upwelling, Arabia indentation and Aegean trench rollback. *Earth and Planetary Science Letters* 375: 254-269.
- Fernandez-Blanco D, Bertotti G, Çiner TA (2013). Cenozoic tectonics of the Tuz Gölü Basin (Central Anatolia Plateau, Turkey). *Turkish Journal of Earth Sciences* 22: 715-738.
- Gailbraith RF (1981). On statistical models for fission track counts. *Mathematical Geology* 13: 471-478.
- Göğüş OH, Pysklywec RN, Şengör AMC, Gün E (2017). Drip tectonics and the enigmatic uplift of the Central Anatolian Plateau. *Nature Communications* 8: 1538.
- Govers R, Fichtner A (2016). Signature of slab fragmentation beneath Anatolia from full-waveform tomography. *Earth and Planetary Science Letters* 450: 10-19.
- Gürbüz A, Saraç G, Yavuz N (2019). Paleoenvironments of the Cappadocia region during the Neogene and Quaternary, central Turkey. *Mediterranean Geoscience Reviews* 1: 271-296.
- Haq BU, Hardenbol J, Vail R (1987). Chronology of fluctuating sealevels since the Triassic (250 million years ago to present). *Science* 235: 1156-1167.
- Helvacı C, Öztürk YY, Satır M, Shang CK (2014). U-Pb zircon and K-Ar geochronology reveal the emplacement and cooling history of the Late Cretaceous Beypazarı granitoid, central Anatolia, Turkey. *International Geology Review* 56: 1138-1155.

- Huvaz O (2009). Comparative petroleum systems analysis of the interior basins of Turkey: Implications for petroleum potential. *Marine and Petroleum Geology* 26: 1656-1676.
- Innocenti F, Agostini S, Di Vincenzo G, Doglioni C, Manetti P et al. (2005). Neogene and Quaternary volcanism in Western Anatolia: Magma sources and geodynamic evolution. *Marine Geology* 221: 397-421.
- Kaymakçı N, Özçelik Y, White SH, Van Dijk PM (2009). Tectono-stratigraphy of the Çankırı Basin: Late Cretaceous to early Miocene evolution of the Neotethyan Suture Zone in Turkey. In: Van Hinsbergen DJJ, Edwards MA, Govers R (editors). *Collision and Collapse at the Africa–Arabia–Eurasia Subduction Zone*. The Geological Society Special Publication (Book 311). London, UK: The Geological Society of London, pp. 67-106.
- Keskin M (2003). Magma generation by slab steepening and breakoff beneath a subduction accretion complex: an alternative model for collision-related volcanism in Eastern Anatolia, Turkey. *Geophysical Research Letters* 30: 8046.
- Ketchum R (2005). Forward and inverse modeling of low temperature thermochronometry data. In: Reiners W, Ehlers TA, Zeitler K (editors). *Thermochronology. Reviews in Mineralogy and Geochemistry* 58: 275-314.
- Lüttig G, Steffens P (1976). Paleogeographic atlas and explanatory notes for Turkey from the Oligocene to the Pleistocene. Hannover, Germany: Bundesanstalt für Geowissenschaften und Rohstoffe, p. 64.
- Maden Tetkik ve Arama Genel Müdürlüğü (2011). Geological map of Turkey 1: 1 250 000 scale, one sheet, Ankara. <http://www.mta.gov.tr/eng/maps/geological-1250000>.
- Öğretmen N, Cipollari P, Frezza V, Faranda C, Karanika K et al. (2018). Evidence for 1.5 km of uplift of the Central Anatolian Plateau's southern margin in the last 450 kyr and implications for its multiphased uplift history. *Tectonics* 37: 359-390.
- Okay AI, Satır M, Zattin M, Cavazza W, Topuz G (2008). An Oligocene ductile strike-slip shear zone: Uludağ Massif, northwest Turkey – implications for the escape tectonics. *Geological Society of America Bulletin* 120: 893-911.
- Okay AI, Zattin M, Cavazza W (2010). Apatite fission-track data for Miocene Arabia-Eurasia collision. *Geology* 38: 35-38.
- Okay AI, Altın D, Kylander-Clark ARC (2019). Major Late Cretaceous mass flows in central Turkey recording the disruption of the Mesozoic continental margin. *Tectonics* 38: 960-989.
- Okay AI, Sunal G, Sherlock S, Kylander-Clark ARC, Özcan E (2020). İzmir-Ankara suture as a Triassic to Cretaceous plate boundary—Data from central Anatolia. *Tectonics* 38. doi: 10.1029/2019TC005849
- Özcan E, Özcan Z, Okay AI, Akbayram K, Hakyemez A (2020). The Ypresian-to Lutetian marine record in NW Turkey: a revised biostratigraphy and chronostratigraphy and implications for Eocene paleogeography. *Turkish Journal of Earth Sciences* 29: 1-27.
- Öztürk YY, Helvacı C, Satır M (2012). Geochemical and isotopic constraints on petrogenesis of the Beypazarı Granitoid, NW Ankara, western central Anatolia, Turkey. *Turkish Journal of Earth Sciences* 21: 53-77.
- Reilinger R, McClusky S, Vernant P, Lawrence S, Ergintav S et al. (2006). GPS constraints on continental deformation in the Africa-Arabia-Eurasia continental collision zone and implications for the dynamics of plate interactions. *Journal of Geophysical Research* 111: B05411.
- Ring U, Johnson C, Hetzel R, Gessner K (2003). Tectonic denudation of a Late Cretaceous-Tertiary collisional belt: regionally symmetric cooling patterns and their relation to extensional faults in the Anatolide belt of western Turkey. *Geological Magazine* 140: 421-441.
- Saraç G (2003). Vertebrate fossil beds of Turkey (in Turkish). Report of the Maden Tetkik ve Arama Genel Müdürlüğü, No. 10609. Ankara, Turkey: MTA Genel Müdürlüğü, p. 218.
- Sarıkaya MA, Çiner A, Zreda M, Şen E, Ersoy O (2019). Chlorine degassing constrained by cosmogenic ³⁶Cl and radiocarbon dating of early Holocene rhyodacitic lava domes of Erciyes Stratovolcano, central Turkey. *Journal of Volcanology and Geothermal Research* 369: 263-275.
- Schildgen TF, Yıldırım C, Cosentino D, Strecker MR (2014). Linking slab break-off, Hellenic trench retreat, and uplift of the Central and Eastern Anatolian plateaus. *Earth-Science Reviews* 128: 147-168.
- Schleiffarth WK, Darin MH, Reid MR, Umhoefer PJ (2018). Dynamics of episodic Late Cretaceous–Cenozoic magmatism across Central to Eastern Anatolia: New insights from an extensive geochronology compilation. *Geosphere* 14: 1990-2008.
- Şen S, Delfino M, Kazancı N (2017). Çeştepe, a new early Pliocene vertebrate locality in Central Anatolia and its stratigraphic context. *Annales de Paléontologie* 103: 149-163.
- Şen Ş, Rage JC (1979). Pliocene vertebrate fauna of Çalta (Ankara). *Bulletin of the Geological Society of Turkey* 22: 155-160 (in Turkish).
- Steininger FF, Berggren WA, Kent, DV, Bernor RL, Şen S et al. (1996). Circum-Mediterranean Neogene (Miocene and Pliocene) marine continental chronologic correlations of European mammal units. In: Bernor RL, Fahlbusch V, Mittmann H-W (editors). *The Evolution of Western Eurasian Neogene Mammal Faunas*. New York, NY, USA: Columbia University Press, pp. 7-46.
- Tari G, Fallah M, Kosi W, Floodpage J, Baur J et al. (2015). Is the impact of the Messinian Salinity Crisis in the Black Sea comparable to that of the Mediterranean? *Marine and Petroleum Geology* 66: 135-148.
- Türkecan A (2015). Cenozoic volcanic rocks of Turkey. Maden Tetkik ve Arama Genel Müdürlüğü, Special Publication No. 33. Ankara, Turkey: MTA Genel Müdürlüğü, p. 258.
- Yıldırım C, Melnick D, Ballato P, Schildgen TF, Echter H et al. (2013). Differential uplift along the northern margin of the Central Anatolian Plateau: inferences from marine terraces. *Quaternary Science Reviews* 81: 12-28.